

**SERI/TP-253-2157**  
**UC Category: 59c**  
**DE8400096**

# **Effects of Soil Conditions on Solar Pond Performance**

**Cecile Leboeuf**  
**David H. Johnson**

**January 1984**

To be presented at  
American Society of Mechanical Engineers  
Solar Energy Division  
Sixth Annual Technical Conference  
8-12 April 1984  
Las Vegas, Nevada

**Prepared under Task No. 1424.00**  
**FTP No. 149**

## **Solar Energy Research Institute**

A Division of Midwest Research Institute

1617 Cole Boulevard  
Golden, Colorado 80401

Prepared for the  
**U.S. Department of Energy**  
Contract No. DE-AC02-83CH10093

Printed in the United States of America  
Available from:  
National Technical Information Service  
U.S. Department of Commerce  
5285 Port Royal Road  
Springfield, VA 22161  
Price:  
Microfiche A01  
Printed Copy A02

**NOTICE**

This report was prepared as an account of work sponsored by the United States Government. Neither the United States nor the United States Department of Energy, nor any of their employees, nor any of their contractors, subcontractors, or their employees, makes any warranty, express or implied, or assumes any legal liability or responsibility for the accuracy, completeness or usefulness of any information, apparatus, product or process disclosed, or represents that its use would not infringe privately owned rights.

## EFFECT OF SOIL CONDITIONS ON SOLAR POND PERFORMANCE

C.M. Leboeuf  
D.H. Johnson

Solar Energy Research Institute  
Golden, Colorado

## ABSTRACT

A recent effort to design a one-acre solar pond at the U.S. Air Force Academy brought up several research issues pertaining to solar pond performance prediction. This report addresses those issues. Interactions of the pond with the soil below it have historically been estimated using very simplistic techniques that tend to ignore soil composition, moisture content, and the coupled heat and moisture transport phenomena. This study examines the models of soil thermal conductivity and heat and mass transport in soils under imposed temperature gradients to assess the potential applicability of these models to solar pond modeling. In addition, a computer simulation code is developed that incorporates the soil thermal conductivity model. Using the code, a parametric analysis was performed illustrating the impact of this property on pond behavior and the importance of experimental model verification for the range of soil temperatures experienced in solar ponds. Implications of the combined heat and moisture movement theory on solar pond performance are presented.

## NOMENCLATURE

$c_l$	specific heat of liquid water ( $J\ kg^{-1}\ ^\circ C^{-1}$ )	$L$	latent heat of vaporization ( $J\ kg^{-1}$ )
$D_T$	isothermal moisture diffusivity ( $D_T = D_{Tl} + D_{Tv}$ , $m^2\ s^{-1}\ ^\circ C^{-1}$ )	$\vec{q}_h$	heat flux ( $W\ m^{-2}$ )
$D_\theta$	thermal moisture diffusivity ( $D_\theta = D_{\theta l} + D_{\theta v}$ , $m^2\ s^{-1}$ )	$\vec{q}_m$	moisture flux ( $kg\ m^{-2}\ s^{-1}$ )
$D_{\theta v}$	isothermal vapor diffusivity ( $m^2\ s^{-1}$ )	$T$	temperature ( $^\circ C$ )
$g_a$	shape factor for the air-filled pores (dimensionless)	$W_a$	air weighting factor (dimensionless)
$g_i$	shape factor for the $i$ th soil component (dimensionless)	$W_i$	weighting factor for the $i$ th soil component (dimensionless)
$h$	relative humidity of air-filled pores (dimensionless)	$X_a$	volume fraction of air in the soil ( $m^3\ m^{-3}$ )
$K$	hydraulic conductivity ( $m\ s^{-1}$ )	$X_i$	volume fraction of the $i$ th soil component ( $m^3\ m^{-3}$ )
		$X_r$	soil field capacity ( $m^3\ m^{-3}$ )
		$X_w$	volume fraction of water in the soil ( $m^3\ m^{-3}$ )
		$\theta_l$	volumetric liquid moisture content in the soil ( $m^3\ m^{-3}$ )
		$\lambda$	effective soil thermal conductivity ( $W\ m^{-1}\ ^\circ C^{-1}$ )
		$\lambda_a$	thermal conductivity of air ( $W\ m^{-1}\ ^\circ C^{-1}$ )
		$\lambda_{ap}$	apparent thermal conductivity of the air-filled pores ( $W\ m^{-1}\ ^\circ C^{-1}$ )
		$\lambda_i$	thermal conductivity of the $i$ th soil component ( $W\ m^{-1}\ ^\circ C^{-1}$ )
		$\lambda_v$	thermal conductivity due to vapor latent heat transfer ( $W\ m^{-1}\ ^\circ C^{-1}$ )
		$\lambda_v^s$	latent heat transfer effect in pores with 100% relative humidity ( $W\ m^{-1}\ ^\circ C^{-1}$ )
		$\lambda_w$	thermal conductivity of water ( $W\ m^{-1}\ ^\circ C^{-1}$ )
		$\rho_l$	density of liquid water ( $kg\ m^{-3}$ )
		$\phi$	soil porosity (dimensionless)

**INTRODUCTION**

Moving ground water will often be present at some depth below the bottom of a solar pond. Heat will be conducted from the pond through the soil to the ground water and hence transported away from the pond. Thus, the thermal conductivity of the soil below a solar pond is an important factor in determining its performance. Previous studies of the thermal performance of solar ponds have considered soil thermal conductivity to be independent of temperature and have usually used values near that of pure water ( $\approx 0.6 \text{ W m}^{-1} \text{ }^\circ\text{C}^{-1}$ ) (1). However, soil conductivity depends on porosity, moisture content, soil makeup, and temperature. In addition, heat and moisture fluxes in the ground may be coupled. A flux of heat caused by a temperature gradient can cause a flux of moisture. The resulting redistribution of moisture will affect the local thermal conductivity.

This paper uses a previously developed model of solar pond thermal performance (2) modified to include a widely accepted model of soil thermal conductivity (3) to assess the effects of soil temperature, moisture content, and makeup on performance. In addition a recognized theory of coupled heat and moisture transport (4) is used to determine the conditions under which the temperature gradients that typically exist below a solar pond might affect the distribution of moisture. The paper concludes with a summary of results and recommendations for further work.

**THEORY**

**Solar Pond Thermal Performance**

The two-dimensional version of SOLPOND (2), a simulation program for salinity gradient solar ponds, was used in this study. This program models the transient thermal performance of a solar pond using the lumped parameter electrical circuit analogy as depicted in Figure 1. Absorption of solar radiation within each element is modeled by a current source. The current source in the storage layer also accounts for the energy delivered by the pond. The user supplies the following inputs: upper convection layer, nonconvecting layer, and storage layer depths; weather data; load data; optical transmission; simulation time step; thermal conductivities; and heat capacities. The upper convecting layer and the storage layer are each described by a single node. The number of nodes used to model the gradient layer and ground are selected by the user. To avoid numerical over stability, implicit finite difference equations compute the time solution. Dynamics of the nonconvecting layer are not modeled. It is assumed that the pond storage temperature never exceeds  $100^\circ\text{C}$  and that excess energy is extracted when necessary to avoid overheating.

**Soil Thermal Conductivity**

A widely accepted and experimentally verified physical model for soil thermal conductivity was developed by de Vries (3). This model assumes that soil is made up of grains of solid materials imbedded in a continuous medium, which is either water or air. In partially saturated soils, water is the continuous medium with pockets of air imbedded in it. In very dry soils (less than 5% moisture content by volume), air is considered the continuous medium with drops of water imbedded in it. The effective soil thermal conductivity for a partially saturated soil is defined as

$$\lambda = \frac{X_w \lambda_w + \sum_{i=1}^n W_i X_i \lambda_i + W_a X_a \lambda_a}{X_w + \sum_{i=1}^n W_i X_i + W_a X_a} \quad (1)$$

where  $n$  is the number of individual solid constituents;  $\lambda_w$ ,  $\lambda_a$ , and  $\lambda_i$  are the thermal conductivities of the water, air, and solid particles, respectively.  $W_i$  and  $W_a$  are weighting factors; and  $X_w$ ,  $X_i$ , and  $X_a$  are the volume fractions of water, soil particles, and air, respectively.

The three main classifications of soil constituents are clay and silt ( $\lambda_1 = 2.93 \text{ W m}^{-1} \text{ }^\circ\text{C}^{-1}$ ), quartz and sand ( $\lambda_2 = 8.79 \text{ W m}^{-1} \text{ }^\circ\text{C}^{-1}$ ), and organic matter ( $\lambda_3 = 0.25 \text{ W m}^{-1} \text{ }^\circ\text{C}^{-1}$ ). Thermal conductivities of water and air are both functions of temperature, according to the following expressions:

$$\lambda_w = 0.55 + 2.34 \times 10^{-3} T - 1.1 \times 10^{-5} T^2; \quad (2)$$

and

$$\lambda_a = 0.0237 + 6.41 \times 10^{-5} T, \quad (3)$$

where  $T$  is the temperature in  $^\circ\text{C}$  and  $\lambda_w$  and  $\lambda_a$  are in  $\text{W m}^{-1} \text{ }^\circ\text{C}^{-1}$ .

The weighting factors depend on the orientation and distribution of soil granules and air pockets. These are assumed to be randomly distributed and oriented ellipsoids such that:

$$W_i = \frac{1}{3} \left[ \frac{2}{1 + \left(\frac{\lambda_i}{\lambda_w} - 1\right) g_i} + \frac{1}{1 + \left(\frac{\lambda_i}{\lambda_w} - 1\right) (1 - 2g_i)} \right] \quad (4)$$

and

$$W_a = \frac{1}{3} \left[ \frac{2}{1 + \left(\frac{\lambda_{ap}}{\lambda_w} - 1\right) g_a} + \frac{1}{1 + \left(\frac{\lambda_{ap}}{\lambda_w} - 1\right) (1 - 2g_a)} \right], \quad (5)$$

where  $g_i$  and  $g_a$  are shape factors corresponding to the soil granules and air pockets, respectively, and  $\lambda_{ap}$  is the apparent thermal conductivity of the air-filled pores.

The shape factors are difficult to determine because of the unpredictable variability in soil structure and pore size; hence they pose a major uncertainty in computing weighting factors. The empirically determined value of  $g_i$  is 0.25 for most soils. The air shape factor is based on the work of de Vries (5), which split the soil into two regions by moisture content. When volumetric moisture content is above the soil field capacity  $X_r$  (the volumetric moisture content retained by the soil after flooding),  $g_a$  is defined as

$$g_a = 0.333 - 0.298 \frac{X_a}{\phi}, \quad (6)$$

where  $\phi$  is the porosity (the ratio of the soil bulk density to the average density of the soil materials). Below field capacity,  $g_a$  is defined as

$$g_a = 0.013 + \frac{X_w}{X_r} (g'_a - 0.013), \quad (7)$$

where  $g'_a$  is the value for  $g_a$  resulting from Eq. 6 when the volumetric moisture content is exactly equal to the field capacity.

The apparent thermal conductivity of the air-filled pores is defined as

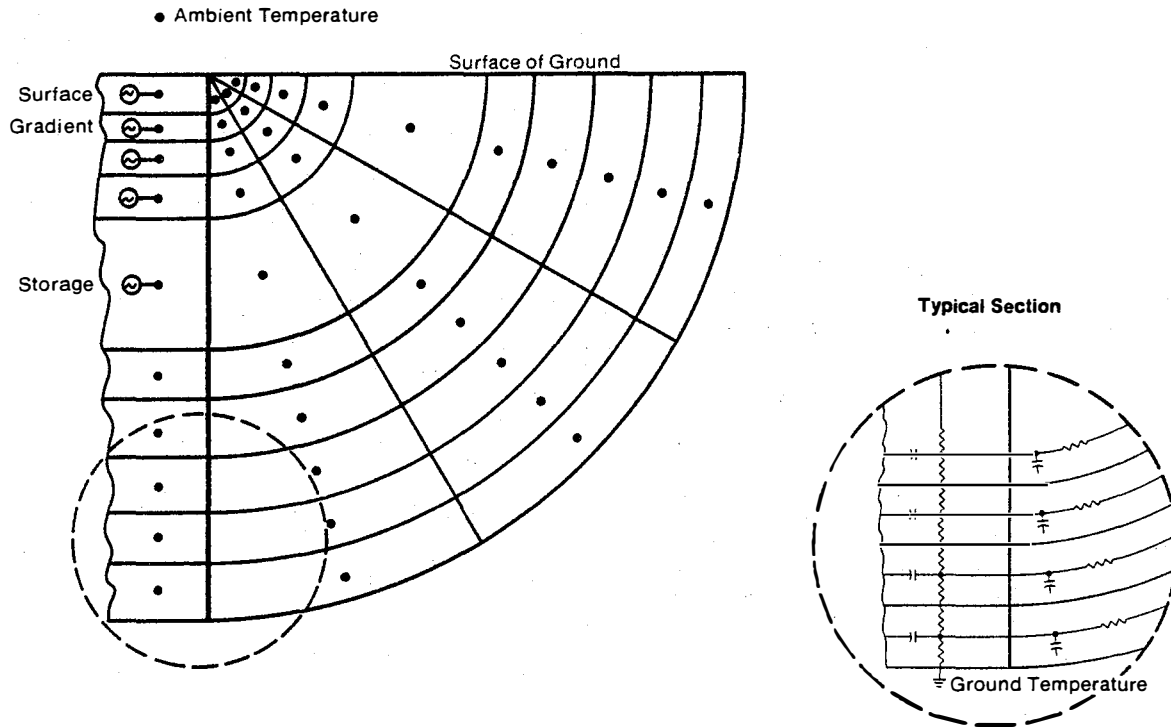


Figure 1. Thermal Model Schematic of Three-Dimensional Solar Pond

$$\lambda_{ap} = \lambda_a + \lambda_v, \quad (8)$$

where  $\lambda_v$  is the thermal conductivity due to vapor latent heat transfer. The value of  $\lambda_v$  depends on the degree of saturation of the air-filled pores, and is given as

$$\lambda_v = h\lambda_v^s, \quad (9)$$

where  $h$  is the relative humidity in the air-filled pores, expressed as a fraction, and  $\lambda_v^s$  is the latent heat transfer due to vapor flow when the relative humidity of the pores is 100%. de Vries (5) presents data on the value of  $\lambda_v^s$  as a function of temperature which can be fitted with the following exponential expression (6):

$$\lambda_v^s = 0.0223 \exp(0.0568 T). \quad (10)$$

**Coupled Heat and Moisture Transport**

Although none of the existing theories completely describes the behavior of coupled moisture and heat transport in soils, several have been verified for certain field conditions. A widely accepted theory was developed by Philip and de Vries (4). This theory considers that a flux of moisture  $\vec{q}_m$  in the soil is caused by the action of gravity and gradients of temperature  $T$  and moisture content  $\theta_l$  so that

$$\frac{\vec{q}_m}{\rho_l} = -D_\theta \vec{\nabla} \theta_l - D_T \vec{\nabla} T + K \vec{k}, \quad (11)$$

where  $\rho_l$  is the density of liquid water,  $D_\theta$  is the isothermal moisture diffusivity,  $D_T$  is the thermal moisture diffusivity, and  $K$  is the hydraulic conductivity. Similarly, a flux of heat  $\vec{q}_h$  in the soil is caused by

a gradient in temperature and moisture content and by the sensible heat carried by a flux of moisture so that

$$\vec{q}_h = \lambda \vec{\nabla} T - \rho_l L D_{\theta v} \vec{\nabla} \theta_l + C_l (T - T_0) \vec{q}_m, \quad (12)$$

where  $L$  is the latent heat of vaporization,  $C_l$  is the specific heat of liquid water,  $D_{\theta v}$  is the isothermal vapor diffusivity, and  $T_0$  is the reference temperature.

**PARAMETRIC STUDIES**

**Effect of Temperature, Moisture Content, and Soil Make-Up on Thermal Conductivity of Soils**

In the theory section, we defined three temperature-dependent variables ( $\lambda_a$ ,  $\lambda_w$ , and  $\lambda_v$ ) that influence the effective soil thermal conductivity. These parameters are plotted versus temperature in Figure 2. The  $\lambda_v^s$  curve crosses the  $\lambda_w$  curve at 60°C and rises sharply thereafter, indicating the dominance of vapor heat transport in the air-filled pores at elevated temperatures. The theory of soil thermal conductivity has traditionally been applied to soils below 40°, such as encountered in agricultural applications or analysis of buried transmission cables. Solar ponds, however, are designed to operate with storage zone temperatures approaching 100°C. The dearth of thermal conductivity data for soils above 40°C, together with the radical difference in the relationship of the temperature-dependent variables in this range, makes it imperative that the de Vries model be verified under solar pond operating conditions before designs are based on it.

The effects of moisture content, soil makeup, and temperature on thermal conductivity are shown in

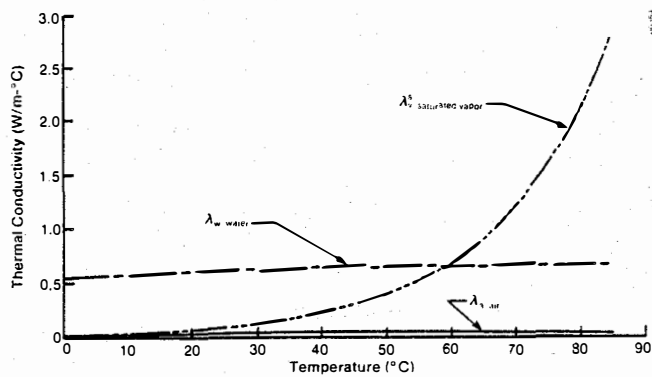


Figure 2. Thermal Conductivity of Air, Water, and Saturated Vapor

Figures 3 and 4. In both figures, the flatness of the curves at 60°C occurs as a result of the cross-over of  $\lambda_w$  and  $\lambda_s$  as shown in Figure 2. At 80°C, the vapor transport is dominant, so that as the pores become filled with water, the effective conductivity actually decreases. The sandy soil shown in Figure 3 has a higher overall thermal conductivity than the finer-grained clayey soil shown in Figure 4, with a maximum value at 80°C and 25% saturation of  $3.8 \text{ W m}^{-1} \text{ }^\circ\text{C}^{-1}$ . Even the clayey soil conductivity reaches  $2.4 \text{ W m}^{-1} \text{ }^\circ\text{C}^{-1}$  at these conditions, which is approximately 2-1/2 times the conductivity of the same soil at 20°C and the same moisture content.

#### Effects of Soil Conditions on Solar Pond Performance

In performing the following analyses, we kept certain assumptions constant. We chose Colorado Springs, Colo., for the solar pond site. Weather data for Colorado Springs, including daily average dry bulb and incident radiation for a typical year, were derived from hourly statistics on the Ersatz TMY (Typical Meteorological Year) data set, which is available from the National Climatic Center. A 30-day time step was used in all performance simulations. Energy extracted from the pond was measured per unit area. Unless otherwise specified, a constant thermal load of  $30 \text{ W m}^{-2}$  is imposed on each solar pond simulation. The surface convecting layer thickness was assumed to be 0.4 m, and the gradient zone depth was 1.2 m. SOLPOND, a computerized solar pond thermal performance simulation code (2), was used in this study to predict pond behavior. Five ground storage nodes are used, with an assumed infinite capacity sink heat at a temperature of 12°C and a depth of 10 m.

To put the ground heat loss issue into proper perspective, we conducted an analysis of the proportion of heat losses from a pond that are to the ground. We assumed a constant soil thermal conductivity. The annual temperature profile of the pond for a specific configuration and fixed energy extraction rate is one illustrative measure of the effect of pond heat losses on performance. If the pond has no side-wall or ground heat losses (soil thermal conductivity  $\ll 1 \text{ W m}^{-1} \text{ }^\circ\text{C}^{-1}$ ), the temperature profile for the base-case pond (which has a storage zone 2.5 m thick and a thermal energy extraction rate of  $30 \text{ W m}^{-2}$ ) is shown as the uppermost curve of Figure 5. The next curve represents a pond that has negligible edge losses but suffers vertical ground losses to a soil with conductivity of  $1 \text{ W m}^{-1} \text{ }^\circ\text{C}^{-1}$ . (This value is commonly used in performance prediction if no other site-specific soil data

is available.) As the pond becomes smaller, edge losses begin to be significant, as evidenced by the decreased temperature profiles for the 100-m, 30-m, and 10-m diameter ponds. While this does not fully bracket performance (i.e., it could be worse), Figure 5 does provide an indication of the importance of ground heat losses to solar pond performance.

Many space-conditioning or industrial process loads being considered for solar pond applications have a prescribed minimum temperature below which they cannot be served. For this reason it is advantageous to design a pond in which the temperature will not fall below a specified minimum during a typical year. A thick storage zone smooths out variations in ambient conditions and can, therefore, maintain a higher pond minimum temperature than a thin storage zone. However, the maximum temperatures achieved are lower in a pond with a thick storage zone. To examine the effect of ground thermal conductivity on storage zone sizing, we examined soil conductivities ranging from 0.2 to  $2.0 \text{ W m}^{-1} \text{ }^\circ\text{C}^{-1}$  and storage zone thicknesses from 0.5 to 3 m; we then determined the minimum operating temperature of the pond for each set of conditions. These data are shown in Figure 6. As the conductivity increases, the benefits gained by thickening the storage zone tend to decrease. Thus for a site which is known to have a high soil thermal conductivity, heat losses to the ground tend to offset any improvements gained by increasing the storage zone beyond about 2 m for these conditions.

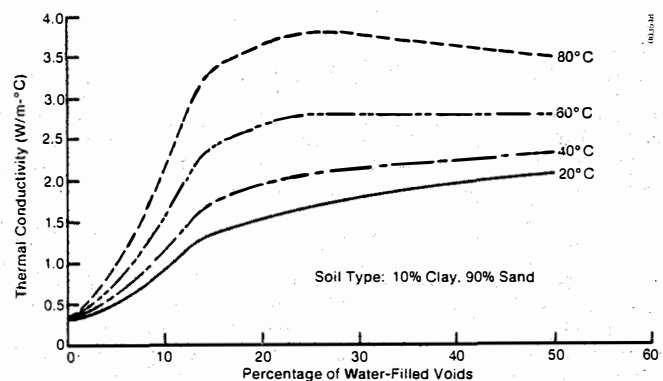


Figure 3. Soil Thermal Conductivity—Sandy Soil

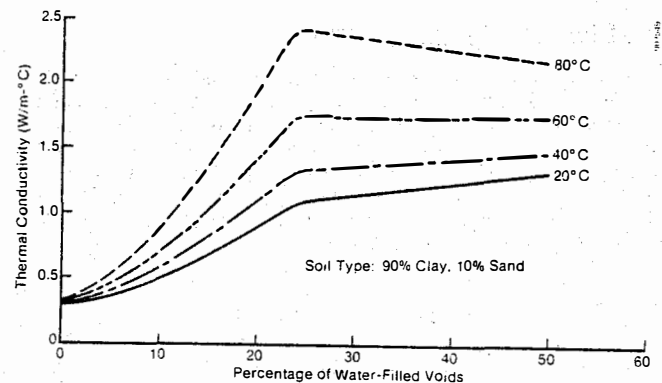


Figure 4. Soil Thermal Conductivity—Clayey Soil

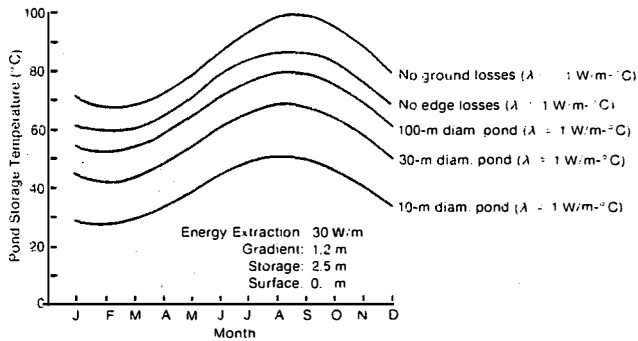


Figure 5. Effect of Ground Thermal Conductivity and Pond Size on Annual Temperature Profile

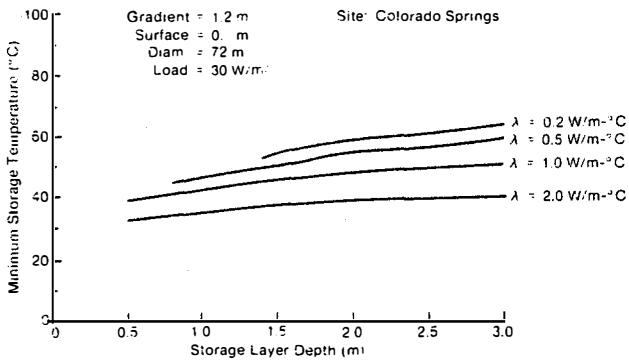


Figure 6. Effect of Ground Thermal Conductivity on Dependence of Minimum Temperature on Storage Layer Depth

The de Vries model for soil thermal conductivity has not been verified in the temperature range of soils beneath solar ponds. It displays some peculiarities in this range because of the exponential nature of the vapor transport term. However, we chose to use the de Vries model with our solar pond thermal performance simulation code to determine the potential impact of a temperature- and moisture-dependent thermal conductivity model on the prediction of solar pond behavior. With the two programs integrated, it is possible to update values of soil thermal conductivity for each of the five ground nodes at each time step, based on nodal temperatures of the preceding iteration. Using two soil types, one sandy (90% sand and 10% clay by weight) and one clayey (90% clay and 10% sand by weight), we have examined solar pond performance for various values of moisture content. The pond performance is measured by its average annual storage temperature in °C (based on a pond with a 0.4-m surface layer, a 1.2-m gradient, a 2.0-m storage zone, and an energy extraction rate of 30 W m<sup>-2</sup>). The moisture content of the soil is shown by percentage of saturation (percentage of void spaces filled with water). Figure 7 shows the relationship between pond storage temperature and soil saturation. As expected, the solar pond on clayey soil maintains a higher temperature than the pond on sandy soil. The average temperature of the pond on clayey soil decreases fairly steeply until the soil moisture content is about 22% of saturation. Beyond 22% of saturation, little drop in average pond temperature is seen. A similar effect is seen for the sandy soil case, but the change in slope of the average temperature first

takes place at about 12% of saturation. From 12% to 22% of saturation, the average temperature drops less steeply. Beyond 22%, the sandy-soil curve also flattens out, but at a level about 7°C lower than the curve for clay.

**Coupled Heat and Moisture Transfer**

We wish to determine the conditions under which the temperature gradient set up in the soil by the presence of a solar pond might cause a redistribution of the soil moisture content from that which existed before the pond was in place. To do this we will determine the impact of an imposed temperature gradient in the soil on the resultant steady-state moisture gradient under conditions of zero moisture flux. In this case, the one-dimensional form of Eq. 11 becomes

$$0 = -D_{\theta} \frac{d\theta_{\lambda}}{dz} - D_T \frac{dT}{dz} + K, \tag{12}$$

or

$$\frac{d\theta_{\lambda}}{dz} = -\frac{D_T}{D_{\theta}} \left( \frac{dT}{dz} + \frac{K}{D_T} \right). \tag{13}$$

Therefore, if the ratio  $K/D_T$  is much less than  $dT/dz$ , then the steady-state temperature gradient will have a profound effect on the steady-state moisture gradient.

Figure 8 shows the behavior of  $K$  as a function of moisture content  $\theta_{\lambda}$  for Yolo light clay at 20°C. Very limited data exist on the temperature dependence of hydraulic conductivity, particularly above 30°C. Figure 9 shows the behavior of  $D_T$  for Yolo clay as a function of volumetric moisture content at 20°C.  $K$  varies considerably, from  $10^{14} \text{ m s}^{-1}$  at  $\theta_{\lambda} = 0.075 \text{ m}^3 \text{ m}^{-3}$  to  $3 \times 10^{-8} \text{ m s}^{-1}$  at  $\theta_{\lambda} = 0.45 \text{ m}^3 \text{ m}^{-3}$ .  $D_T$  is fairly constant in this range of  $\theta_{\lambda}$  at approximately  $2.3 \times 10^{-11} \text{ m}^2 \text{ s}^{-1} \text{ }^{\circ}\text{C}^{-1}$ .

A typical temperature gradient beneath a solar pond is  $23^{\circ}\text{C m}^{-1}$  according to Meyer and Hedstrom (7). Using these values, and for  $\theta_{\lambda}$  up to about 20%,

$$\frac{K}{D_T} < 2.3^{\circ}\text{C m}^{-1} \ll \frac{dT}{dz} = 23^{\circ}\text{C m}^{-1},$$

but for  $\theta_{\lambda}$  greater than about  $0.45 \text{ m}^3 \text{ m}^{-3}$

$$\frac{K}{D_T} > 230^{\circ}\text{C m}^{-1} \gg \frac{dT}{dz} = 23^{\circ}\text{C m}^{-1}.$$

Hence the influence of the temperature gradient on the moisture gradient in the soil will be significant for relatively dry soils but not for relatively wet soils (assuming the soil to be Yolo clay).

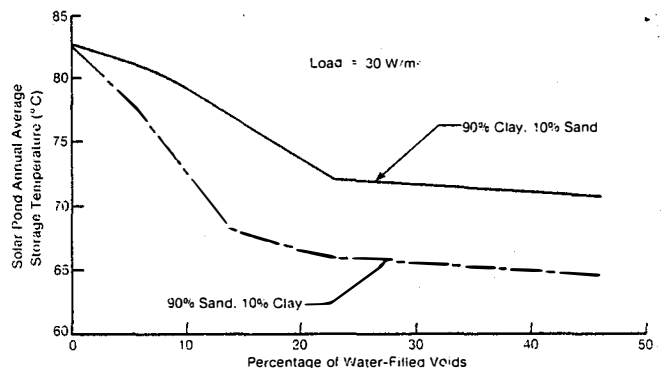


Figure 7. Effect of Moisture Content on Pond Storage Temperature

These results suggest that combined heat and moisture flux may be an important consideration for many solar ponds. Figure 7 shows that for our example, solar pond average annual storage temperature decreased from 83°C to 73°C as the moisture content of underlying soil went from 0% to 20% of saturation for a light clay soil, assuming no interaction between heat flux and moisture distribution. If the temperature gradients set up by a solar pond interact with the moisture content to drive moisture away from the bottom of the pond, then an insulating region of low thermal conductivity might be created below the pond, preventing such a drastic reduction in performance. This possibility remains as speculation until data on soil properties can be obtained at solar pond operating temperatures (~80°C). A literature search by the authors has failed to uncover such data.

#### SUMMARY AND RECOMMENDATIONS

Heat lost through the soil to moving ground water can have a significant effect on solar pond performance. The amount of heat lost will depend on the soil thermal conductivity, which is a function of moisture content, soil makeup, porosity, and temperature. Parametric studies using an accepted model of soil thermal conductivity show that under the range of solar pond operating conditions moisture content, soil makeup, and temperature have significant effects on solar pond performance. However, these results depend on extrapolation of data from approximately 30°C to solar pond operating temperatures near 80°C because sufficient data on soil thermal properties at higher temperatures are not available. It is also possible that the flux of heat from the solar pond through the soil to

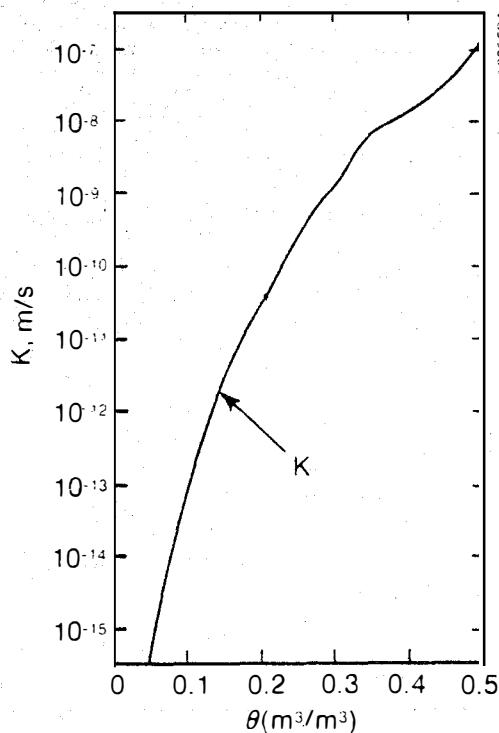


Figure 8. Variation of Hydraulic Conductivity with Moisture Content—Yolo Clay

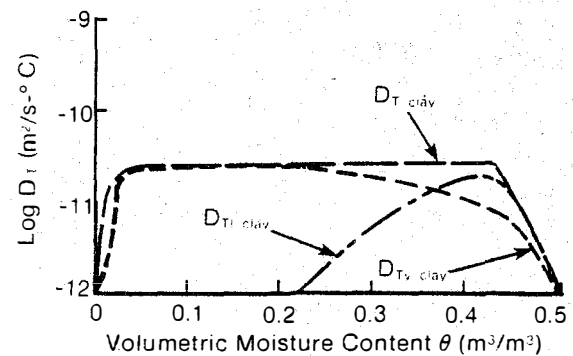


Figure 9. Thermal Moisture Diffusivities for Yolo Clay at 20°C

the ground water may cause a redistribution of moisture in the soil below the pond with a corresponding effect on soil thermal conductivity. This possibility is supported by an accepted theory of coupled heat and moisture transport in soils but also depends on extrapolation of data from about 30°C to solar pond operating temperatures (about 80°C).

A literature search by the authors has failed to uncover sufficient data on soil thermal properties to completely evaluate soil thermal conductivity and coupled heat and moisture movement at solar pond operating conditions. We recommend that such data be obtained because of the potential importance of these subjects in understanding solar pond thermal performance.

#### REFERENCES

1. Jayadev, T. S., and Henderson, J., "Salt Concentration Gradient Solar Ponds—Modeling and Optimization," SERI/TP-35-277, June 1979. Presented at the Annual Meeting of the International Solar Energy Society, Atlanta, GA, May 28-June 1, 1979.
2. Henderson, J., and Leboeuf, C. M., "SOLPOND - A Simulation Program for Salinity Gradient Solar Ponds," SERI/TP-351-559, Jan. 1980. Presented at the Second Annual Systems Simulation and Economics Analysis Conference, San Diego, CA, Jan. 23-25, 1980.
3. de Vries, D. A., "Simultaneous Transfer of Heat and Moisture in Porous Media," Transactions American Geophysical Union, Vol. 39, No. 5, Oct. 1958.
4. Philip, J. R., and de Vries, D. A., "Moisture Movement in Porous Materials Under Temperature Gradients," Transactions American Geophysical Union, Vol. 38, No. 2, Apr. 1957.
5. de Vries, D. A. "Thermal Properties of Soils," Physics of Plant Environment, W. R. Van Wijk, ed., North Holland Publishing Co., Amsterdam, 1963.
6. Walter, W. R., Sabey, J. D., and Hampton, D. R., "Studies of Heat Transfer and Water Migration in Soils," DOE/CS/31039-T1, 1981, Colorado State University, Ft. Collins, CO.
7. Meyer, K. A., and Hedstrom, J. C., "Estimates of Ground Conductivity for the DOE-USAFA Experimental Solar Pond," LA-UR-82-2904, 1982, Los Alamos National Laboratory, Los Alamos, NM.